Numerical analysis on heat transfer and fluid flow for arrays of non-uniform plate length aligned at angles to the flow direction

Received November 1994
Revised January 1996

L.B. Wang and W.Q. Tao
School of Energy and Power Engineering, Xi'an Jiaotong University, Xi'an, Shaanxi 710049, People's Republic of China

Nomenclature

a	=	thermal diffusivity, m^2/s
f	=	friction factor
h	=	heat transfer coefficient, W/m^2 C
k	=	thermal conductivity, W/m C
Lp	=	streamwise length of one cycle, m
L1	=	length of long plate, m
L2	=	length of short plate, m
Nu	=	Nusselt number
p	=	pressure, Pa
Pr	=	Prandtl number
q	=	heat flux, W/m^2
Re	=	Reynolds number
T	=	temperature, C
T_b	=	bulk temperature, C
Tp	=	transverse spacing between two adjacent plates, m
Tw	=	wall temperature, C
u	=	streamwise velocity, m/s
v	=	spanwise velocity, m/s
x	=	streamwise co-ordinate, m
y	=	spanwise co-ordinate, m
δ	=	thickness of plate, m
y	=	distance between two adjacent grids in y-direction, m
θ	=	angle, degree
Θ	=	dimensionless temperature, C
ν	=	fluid kinematics velocity, m^2/s
ρ	=	fluid density, kg/m3
ϕ	=	general dependent variable

Subscripts

m	=	mean
x	=	local

Note: The symbols defined above are subject to alteration on occasion

Introduction

It has been recognized that higher convective heat transfer coefficient can be obtained when an array of plates is aligned at an angle to the flow direction to interrupt the flow periodically. Each interruption enables the velocity and temperature distributions to become more cross-sectionally homogeneous and a new boundary layer is restarted when the plate surface is reattached downstream of the interruption. The slit fins used in the compact heat exchanger and automobile radiators are examples of using this technique. The heat transfer and pressure drop characteristics of this type of flow have been studied by both experimental and numerical methods. Lee (1986, 1989) and Zhang and Lang (1989) experimentally investigated the heat transfer and pressure drop performances of an array of plates aligned at an angle to the flow direction, which serves as a two-dimensional model of louvred fins. Recently, Huang and Tao (1993) performed an experimental study on heat/mass transfer

This work was supported by the Doctorate Foundation of Chinese Institutes and Universities.

International Journal of Numerical Methods for Heat & Fluid Flow
Vol. 7 No. 5, 1997, pp. 479-496.

and pressure drop characteristics for arrays of non-uniform plate length positioned obliquely to the flow direction. It is found that the heat transfer performance of the non-uniform plate length array is generally better than that of uniform plate length array in the Reynolds number range from 1.98×10^2 to 1.66×10^3.

As far as the numerical simulation is concerned, starting from the work conducted by Patankar *et al.*(1977), a limited number of computations have been performed for periodically fully developed laminar flow and heat transfer (Asako and Faghri, 1988; Pang *et al.,* 1990 and Patankar and Prakash, 1981). In the work conducted by Pang *et al.* (1990), the streamwise periodic boundary conditions were implemented by mutual replacements of the field variables at the inlet and outlet boundaries. In order to do that, the streamwise length of the computation domain had to be larger than one cycle; otherwise the solution was difficult to converge. This practice was also adopted in the works performed by Amano (1985) and Xin and Tao (1988).

The purposes of this study are twofold. First, it is designed to investigate numerically the heat transfer performance of the array with non-uniform plate length in the low Reynolds number region, for which the experimental work in the Reynolds number range from 1.98×10^2 to 1.66×10^3 has been conducted by Huang and Tao (1993). To ensure that the flow is laminar, the Reynolds number is limited to below 150. The second purpose is related to numerical algorithm. In the configuration studied by Xin and Tao (1988) and Pang *et al.* (1990), only the streamwise boundary condition was periodic. However, for the array configuration studied in this work, both streamwise and spanwise boundary conditions are periodic. It is the authors' consideration that the numerical analysis for the turbulent flow in such an array configuration be performed with body-fitted coordinates. In that case, if the computation domain is larger than one cycle in both directions, the outflow boundaries for one cycle cannot be found straightforwardly in the transformed plane, which is inconvenient for implementation of the mutual replacement method. Therefore it is desired that for the laminar flow computed in the physical plane, a numerical technique be developed which enables the implementation of the mutual replacement method in a computation domain of one cycle.

Mathematical formulation

The problem analysed in this paper is schematically pictured in Figure 1(a). As seen there, a two-dimensional array of non-uniform plate length with constant temperature T_w is positioned obliquely to the flow direction. The configuration studied can be specified by the following parameters: the periodic axial length L_p, the plate lengths L_1, L_2, the oblique angle θ, the transverse space between the plates T_p, and the plate thickness δ. The engineering background of this study is the heat transfer and fluid flow in louvred fins used in automobile and other low Reynolds number heat exchangers, where the fins are formed by slitting a continuous thin copper plate and then turning the slitted segments to

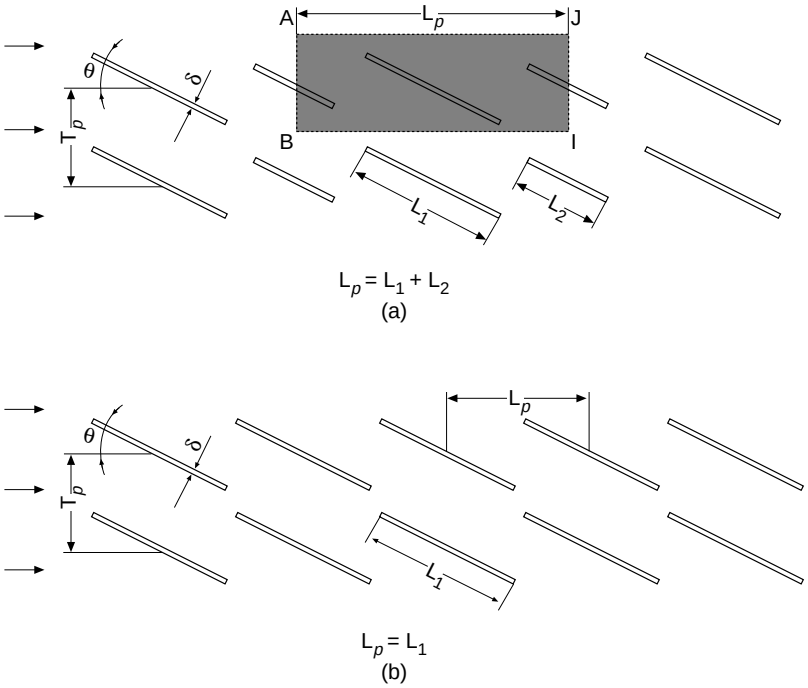

Figure 1.
Schematic diagram of interrupted-plate array (a) with non-uniform plate length; (b) with uniform plate length

an angle. In this case, $L_p = L_1 + L_2$. In order to make the laminar flow analysis consistent with the corresponding experimental work, the geometric parameters used in Huang and Tao (1993) are adopted in this paper, i.e. the plate thickness δ = 1.5mm, the oblique angle θ = 25°, the short plate length L_2 = 15mm, the ratio of L_1/L_2 = 1.5, 2.0, and 2.5, and the transverse pith T_p = 20, 25, and 30mm. Thus nine configurations can be obtained from the combination of the different L_1/L_2 and T_p/L_p (Table I). For simplicity of later writing, a case number is assigned to each configuration.

Case	L_1, mm	T_p, mm	L_p, mm	L_1/L_2	T_p/L_p
1	37.5	30.0	52.5	2.5	0.571
2	30.0	30.0	45.0	2.0	0.667
3	22.5	30.0	37.5	1.5	0.800
4	37.5	25.0	52.5	2.5	0.476
5	30.0	25.0	45.0	2.0	0.556
6	22.5	25.0	37.5	1.5	0.667
7	37.5	20.0	52.5	2.5	0.381
8	30.0	20.0	45.0	2.0	0.444
9	22.5	20.0	37.5	1.5	0.533

Table I.
Characteristics of configurations investigated (L_2 = 15mm, θ = 25°)

In Figure 1(b), an array of uniform plate length is pictured, which serves as a reference array for comparison of heat transfer performed in the later discussion.

The analysis is based on the following assumptions:

- the fluid properties are constant;
- the flow and heat transfer are laminar and periodically fully developed;
- the body force and the dissipation term are neglected.

It should be noted that for the present study one cycle includes two plates, one short and one long. The domain of one cycle is shown by the shaded area in Figure 1(a). The computation domain is shown in Figure 2, where domain ABIJ is just one cycle, while ABCD is one cycle plus one control volume in the x direction. For simplicity, the domain ABCD will be referred to as domain 1, ABIJ as domain 2.

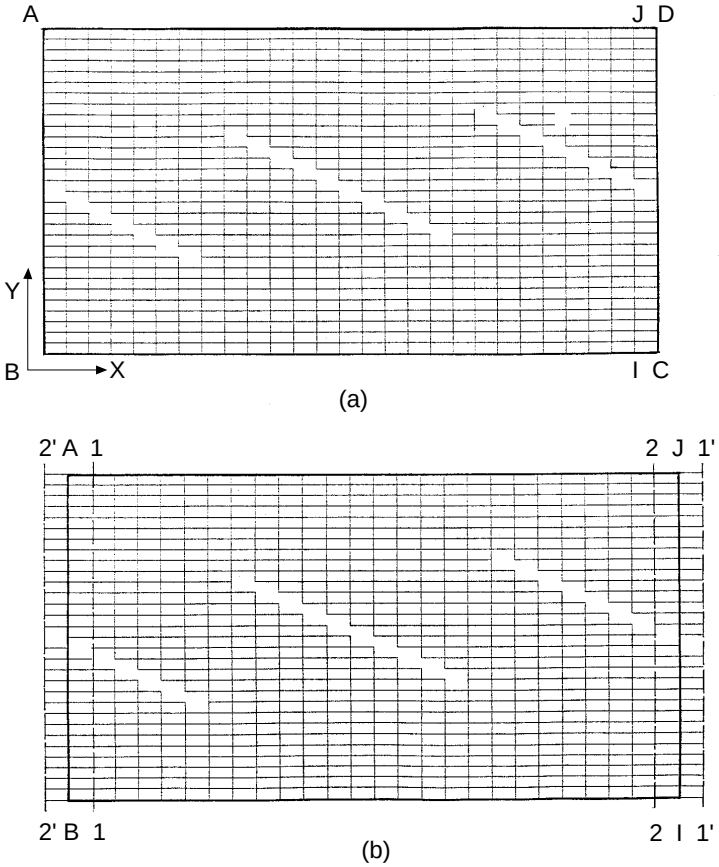

Figure 2.
Solution domain;
(a) domain 1;
(b) domain 2

The fluid flow and heat transfer in the array described above can be specified by the following equations:

continuity equation:

$$\frac{\partial u}{\partial x}+\frac{\partial v}{\partial y}=0 \tag{1}$$

Momentum equations:

$$u\frac{\partial u}{\partial x}+v\frac{\partial u}{\partial y}=-\frac{1}{\rho}\frac{\partial p}{\partial x}+\nu\left(\frac{\partial^2 u}{\partial x^2}+\frac{\partial^2 u}{\partial y^2}\right) \tag{2}$$

$$u\frac{\partial v}{\partial x}+v\frac{\partial v}{\partial y}=-\frac{1}{\rho}\frac{\partial p}{\partial x}+\nu\left(\frac{\partial^2 v}{\partial x^2}+\frac{\partial^2 v}{\partial y^2}\right) \tag{3}$$

Energy equation:

$$u\frac{\partial T}{\partial x}+v\frac{\partial T}{\partial y}=a\left(\frac{\partial^2 T}{\partial x^2}+\frac{\partial^2 T}{\partial v^2}\right) \tag{4}$$

Boundary conditions:

$$T(x,T_p)=T(x,0) \tag{5}$$

$$v(x,T_p)=v(x,0) \tag{6}$$

$$u(x,T_p)=u(x,0) \tag{7}$$

$$\frac{T(0,y)-T_w}{T_b(0)-T_w}=\frac{T(L,y)-T_w}{T_b(L)-T_w} \tag{8}$$

$$v(o,y)=v(L,y) \tag{9}$$

$$u(o,y)=u(L,y) \tag{10}$$

In order to simulate the solid plate in the flow region with zero velocity and uniform temperatures, special attention was paid to assigning the discretization coefficients of the control volume in the solid region, which is outlined in Yang and Tao (1992), and will not be restated here.

Numerical procedure

The governing equations were discretized by the finite volume approach. The flow field was predicted by the SIMPLE algorithm, the details of which can be found in Patankar (1980). The periodic boundary conditions were implemented as follows:

Domain 1

The periodic boundary conditions in x-direction were implemented by mutual replacement of the field variables at inlet and outlet regions, as described by Xin and Tao (1988), the details also can be found in Pang *et al.* (1990). Several choices were tried for the implementation of periodic boundary conditions in y-direction, the following linear interpolation was finally used.

$$\phi(i,1)=\phi(i,M_1)=(\phi^*(i,2)+\phi*(i,M_2))/2 \quad (11)$$

where * represents the previous iteration, and M_1, M_2 are the last and last but one indices in y-direction. This implies that, after each iteration, the arithmetic mean value of $\phi(i, 2)$ and $\phi(i, M_2)$ is assigned to the top and bottom boundaries and serves as the boundary condition for the next iteration.

It should be noted that the periodic boundary conditions in the y direction cannot be implemented by the mutual replacements of the field variables at corresponding periodic boundary regions . This is because, in the y direction, the computation domain is not extended, therefore, a grid in one boundary cannot find its corresponding point within the computation domain, where the dependent variable values are renewed during an iteration. In addition, for the problem investigated here, the flow rate in y direction is not known, and the velocity, v cannot be treated in such a way as that in x direction, in which the Reynolds number can be kept unchanged during the iteration. For this purpose, the inlet u velocities were predetermined after each iteration by multiplying a factor which was the ratio of desired averaged velocity to the current averaged one. Since no constraint of flow rate in y direction should be posed at the top and bottom boundaries, the periodic condition at the two boundaries was implemented by assigning the same value interpolated from second and last but one points in y direction.

Domain 2

For the computational domain ABIJ, since the computation domain in the x and y directions are both not extended, the periodic boundary condition in both x and y directions were implemented in the same way as that for the y direction of domain 1. We may interpret this practice for the x direction in the following way. Imagine that the computation domain ABIJ be extended in x direction by two control volumes, one ahead of the cycle and the other behind its outlet (see Figure 2b). Then, when the iteration process converges, the velocity values at boundary 2'–2' should be equal to that 2–2, and the same is true for the values at 1–1 and 1'–1'. Therefore, we may take the value of the velocities at line 1–1 and line 2–2 as the boundary value at cycle inlet and outlet for the next iteration. As far as the temperature is concerned, the periodic condition is valid only for the dimensionless value. Thus, the dimensionless values determined by equation (12) are taken as the dimensionless temperatures at the cycle inlet and outlet for next iteration.

$$\Theta=\frac{1}{2}\left(\frac{T(x_{1-1},y)-T_w}{T_b(x_{1-1})-T_w}+\frac{T(x_{2-2},y)-T_w}{T_b(x_{2-2})-T_w}\right) \quad (12)$$

where x_{1-1} and x_{2-2} are positions corresponding to the lines 1–1 and 2–2 in Figure 2(b).

The local temperatures at the cycle inlet and outlet can be calculated as:

$$T(o,y)=T_w+\Theta[T_b(0)-T_w] \quad (13)$$

$$T(L,y)=T_w+\Theta[T_b(L)-T_w] \quad (14)$$

Attention is now turned to the definitions of local heat transfer coefficient, Nusselt number, and Reynolds number. The local heat transfer coefficient was determined by the following equation:

$$h_x = q_x / (T_w - T_b(x)) \tag{15}$$

The bulk temperature $T_b(x)$ was defined as

$$T_b(x) = \int^{T_p} T(x,y)u(x,y)dy \Big/ \int^{T_p} u(x,y)dy \tag{16}$$

The local heat flux was computed by Fourier's law of heat conduction. For example, the value of heat flux on surface bc as shown in Figure 3 was determined by:

$$q_{bc} = k[T_w - T(i,j)]/(\Delta y/2) \tag{17}$$

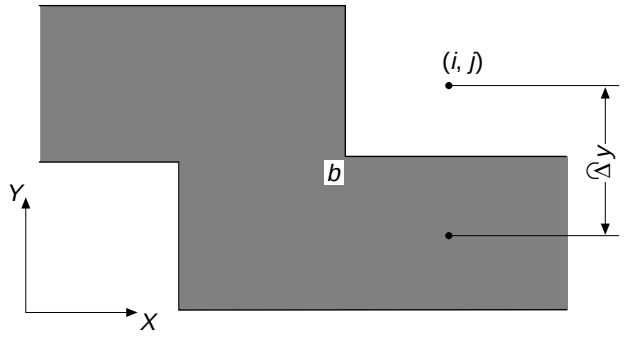

Figure 3.
Diagram used for calculating local heat flux

The average heat transfer coefficient of one cycles was computed by

$$h_m = q_m / \{[T_b(L) - T_b(0)]/(\ln[T_w - T_b(0)] - \ln[T_w - T_b(L)]]\} \tag{18}$$

The Reynolds number and the per-plate Nusselt number were defined as

$$Re = u_m L_2 / v \quad Nu = h_m L_2 / k \tag{19}$$

where the short plate length, L_2, is taken as the characteristic dimension, which is inconsistent with the experimental work of Huang and Tao (1993). The friction factor of one cycle was determined from the following equation:

$$f = [p_m(0) - p_m(L)]/(\rho u_m{}^2/2) \tag{20}$$

A preliminary computation was performed to assure the grid independence of the numerical solution for the case number 1, $Re = (85.7 \times 10)$ with two uniform grid systems in domain 2. The results are shown in Table II. The difference between the two solutions of Nu is 1.75 per cent and of f is 0.55 per cent. As these differences are small, the grid numbers used in the computations for the nine cases are basically in between these two systems (see Table III).

The velocity field convergence criterion used in this study was that the ratio of mass flux residual in each control volume to the inlet mass flow rate was less than 10^{-6}. The two computation domains behave quite differently in

convergence rate. Take case 6 as an example, the iteration times for six Reynolds numbers are listed in Table IV. The iteration in domain 2 converges much faster than that of domain 1. This can be explained by the following consideration: in domain 1, only the downstream information is used for the upstream and vice versa, but in domain 2 the information of both downstream and upstream is combined and then used for both the downstream and upstream boundary conditions.

Table II.
Grid independence study (Case 1, $Re = 100$)

Grid number	*NU*	*f*
40×49	3.6667	1.7158
30×37	3.6025	1.7064

Table III.
Grid sizes

Case	Domain 1	Domain 2
1	40×49	41×49
2	34×49	35×49
3	28×49	29×49
4	40×41	41×41
5	34×41	35×41
6	28×41	29×41
7	40×33	41×33
8	34×33	35×33
9	28×33	29×33

Table IV.
Iteration times of two computation domains

Re	Domain 1	Domain 2
25	646	281
50	648	349
75	736	265
100	836	403
125	915	446
150	1,176	502
237	1,265	523
314	1,308	602
411	1,423	758

Results and discussion

Comparison of results in two computational domains

The difference of the calculation results for *Nu* and *f* conducted in domain 1 and domain 2 are presented in Figure 4 for cases 1, 4 and 7. The maximum difference of *f* is 5.5 per cent, and that of *Nu* is 6.5 per cent. It is interesting to note that for the other six configurations the percentage differences in *Nu* and *f* of the two domains are generally much less than those shown above. Comprehensive comparison between the flow patterns obtained in two domains have been conducted, and it is hard to find even a minor difference between the two counterparts. Lack of space limitation does not allow us to present all of them. For case 1, the velocity vectors and temperature contours are shown in Figures 5 and 6 as an example. It can thus be concluded that the technique developed in this paper for using a computation domain of one cycle is successful.

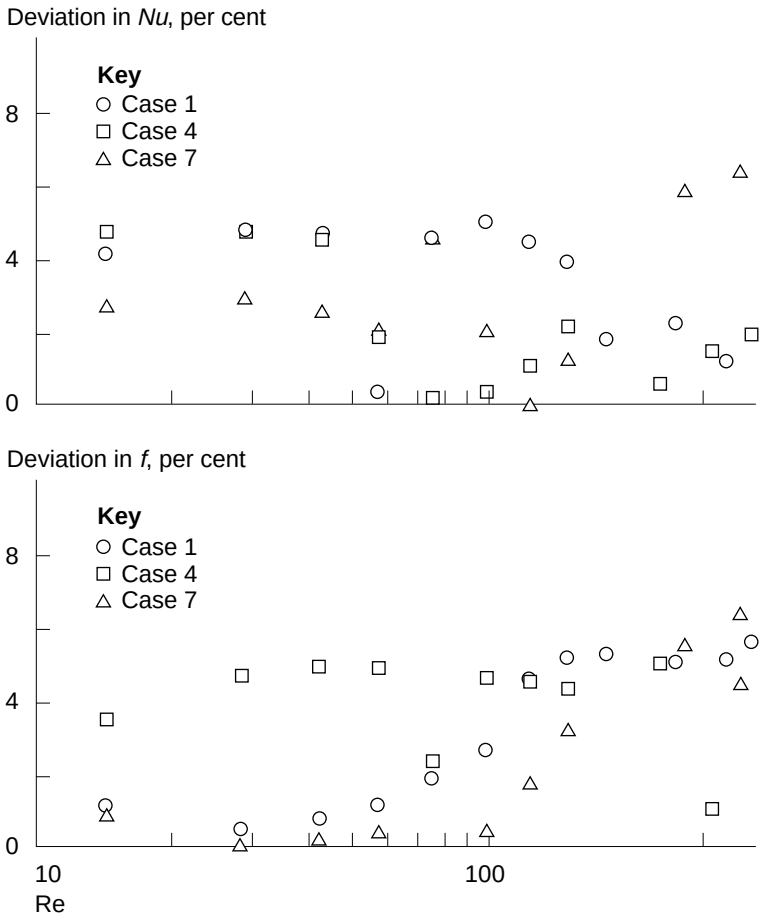

Figure 4.
Percentage deviation in calculation results of *NU* and *f* corresponding to domain 1 and domain 2

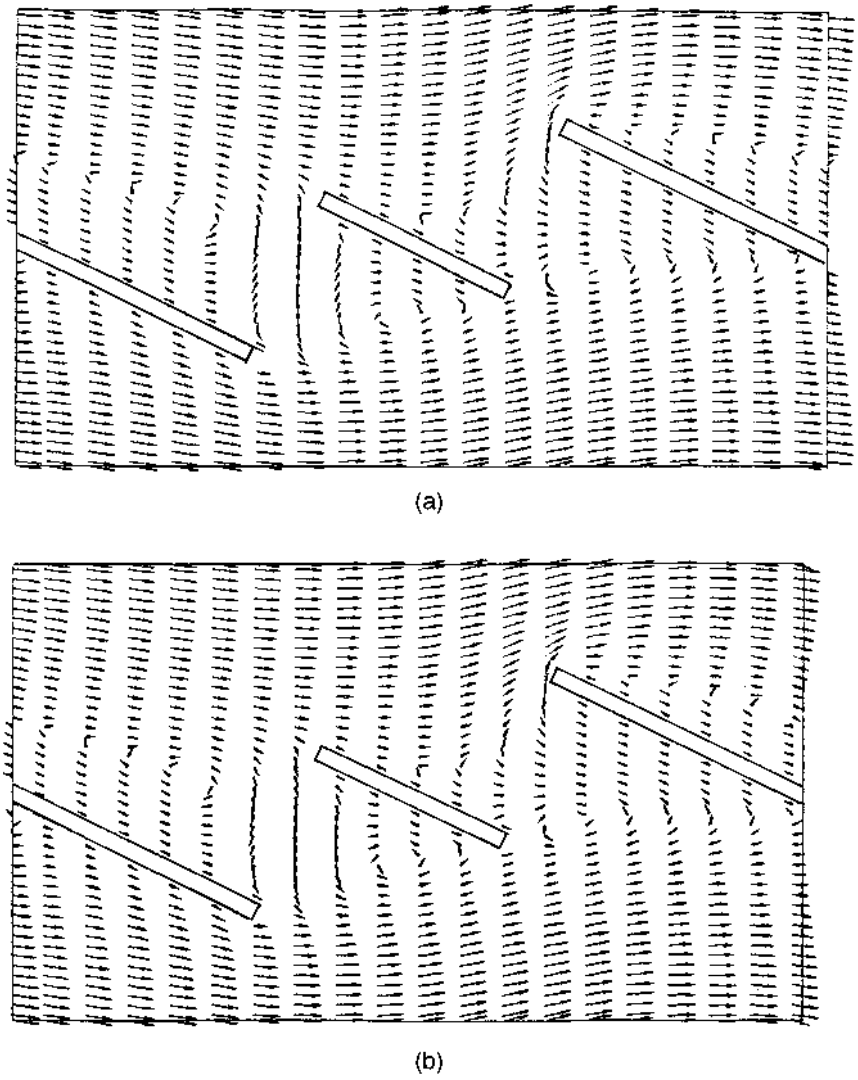

Figure 5.
Velocity fields for case number 1, $Re = 5.0 \times 10$
(a) calculated in domain 1;
(b) calculated in domain 2

Effects of L_1/L_2 and T_p/L_p on the heat transfer and pressure drop characteristics
The per-cycle average Nusselt number and friction factor in the periodically fully developed region are shown in Figures 7 and 8, respectively. It can be seen clearly that at the same transverse pitch, with an increase in L_1/L_2, both the per-cycle average Nusselt number and friction factor increase. While at the same L_1/L_2, with increase in T_p, Nusselt number and friction factor decrease. These variation trends qualitatively agree with the experimental data obtained at higher Reynolds number by Huang and Tao (1993).

The above variation trends may be attributed to the flow pattern difference. As an example, the velocity vectors are shown in Figure 9 for case 7, 8 and 9

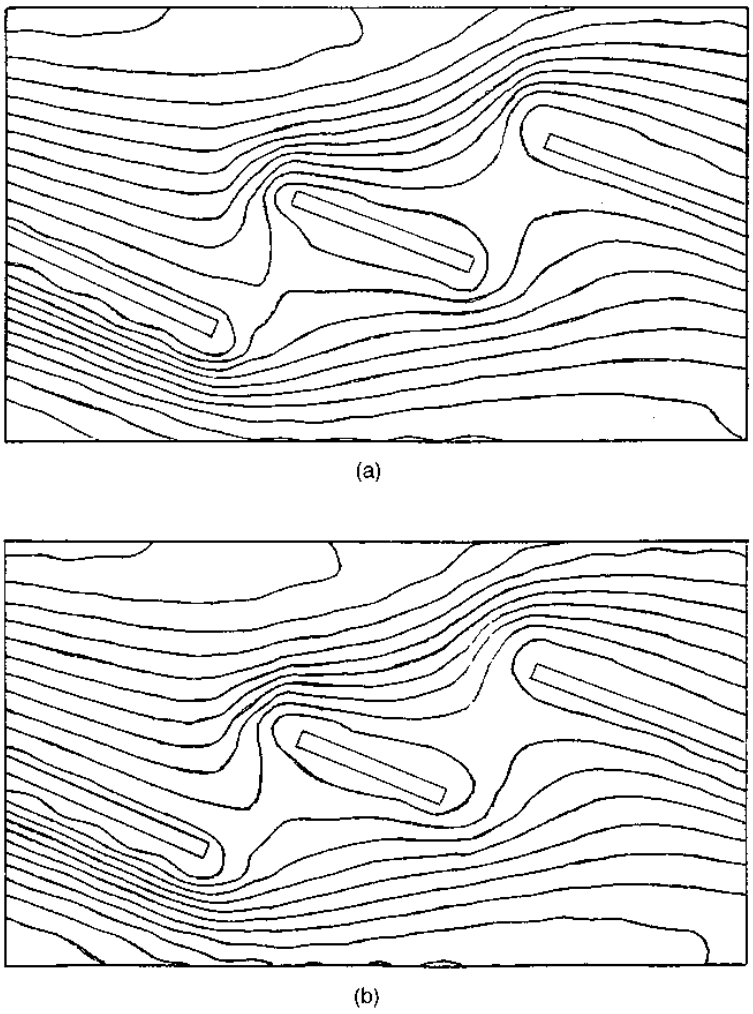

Figure 6.
Temperature fields for case number 1, $Re = 2.5 \times 10$; (a) calculated in domain 1, (b) calculated in domain 2

($Re = 1.0 \times 10^2$, T_p = 20mm). These figures definitely show that with the increase in $L_1/L_2$the recirculation flows between any two successive plates become more intensive, hence enhancing the heat transfer with an inevitable penalty in pressure drop.

Comparison with relevant experimental results

Although the major purpose of the present study is to investigate the feasibility of the linear interpolation technique for the prediction of the periodicality fully developed fluid flow and heat transfer in the one-cycle domain, comparison of the numerical data with the relevant experimental results is also valuable to confirm further the reliability of this technique.

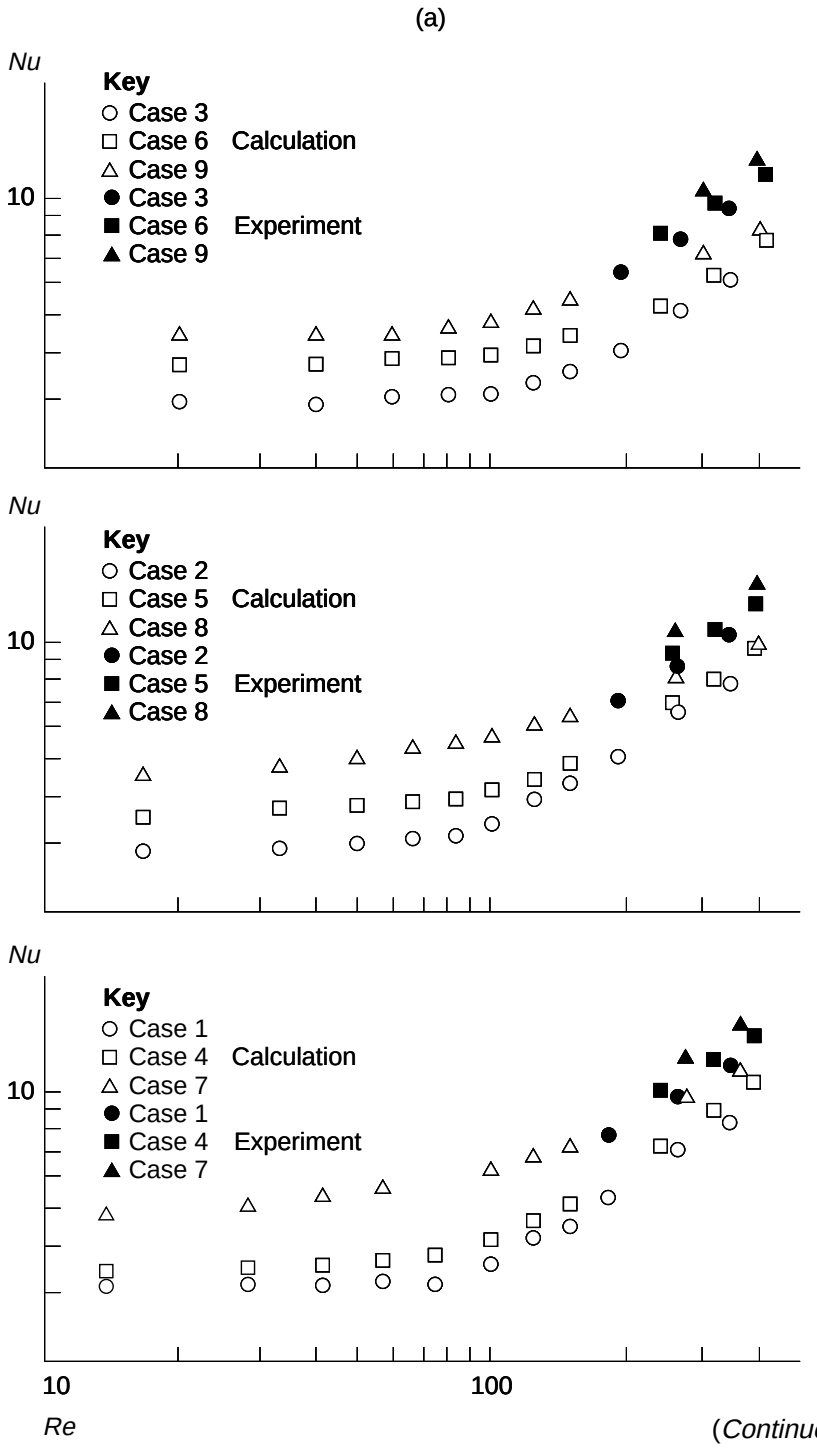

Figure 7.
Calculated results of Nusselt number: (a) effect of the transverse pitch on heat transfer; (b) effect of the ratio of successive plate length on heat transfer

(*Continued*)

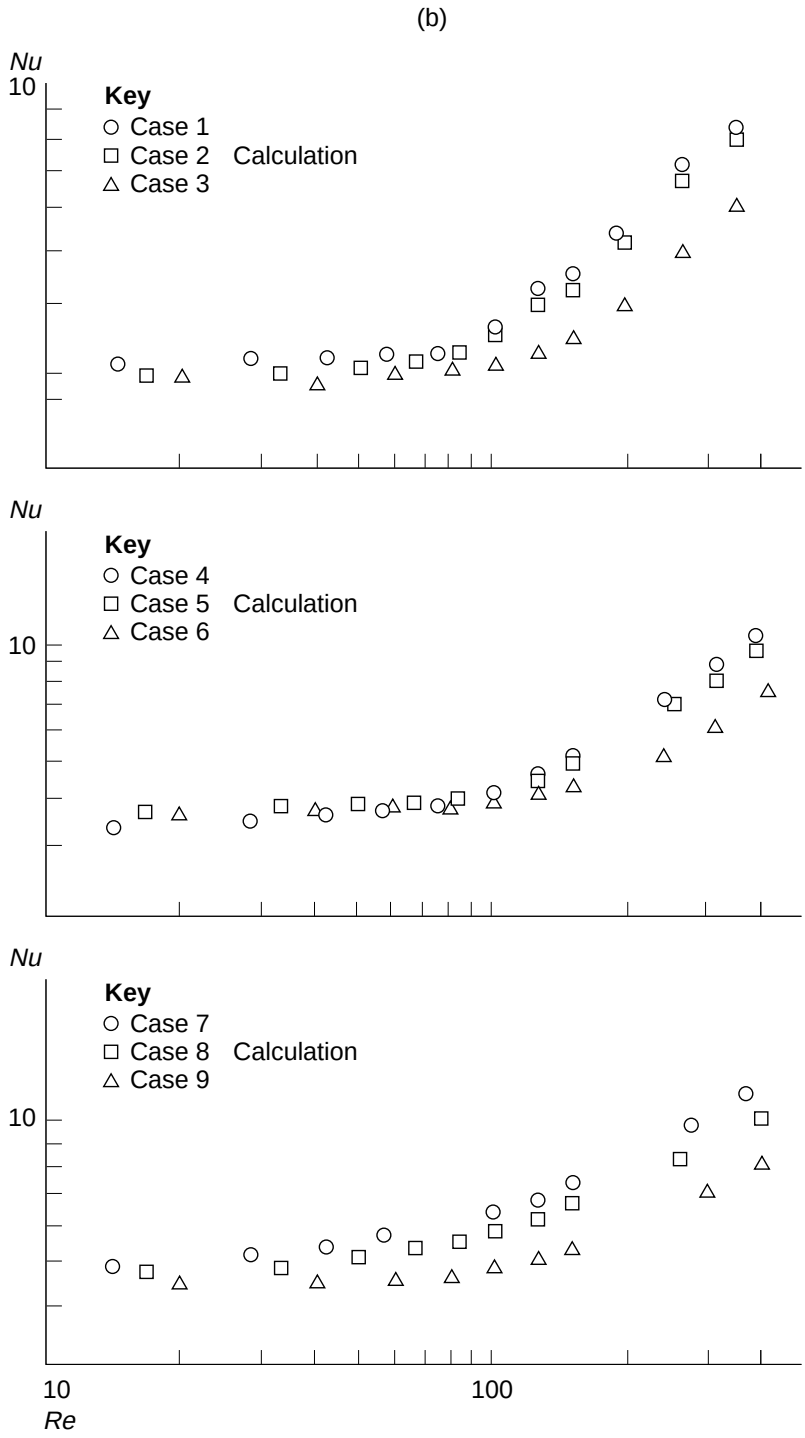
(b)
Nu
10
Key
Case 1
Case 2
Case 3
Calculation
Nu
Key
Case 4
Case 5
Case 6
Calculation
10
Nu
Key
Case 7
Case 8
Case 9
Calculation
10
10
100
Re

Figure 7.

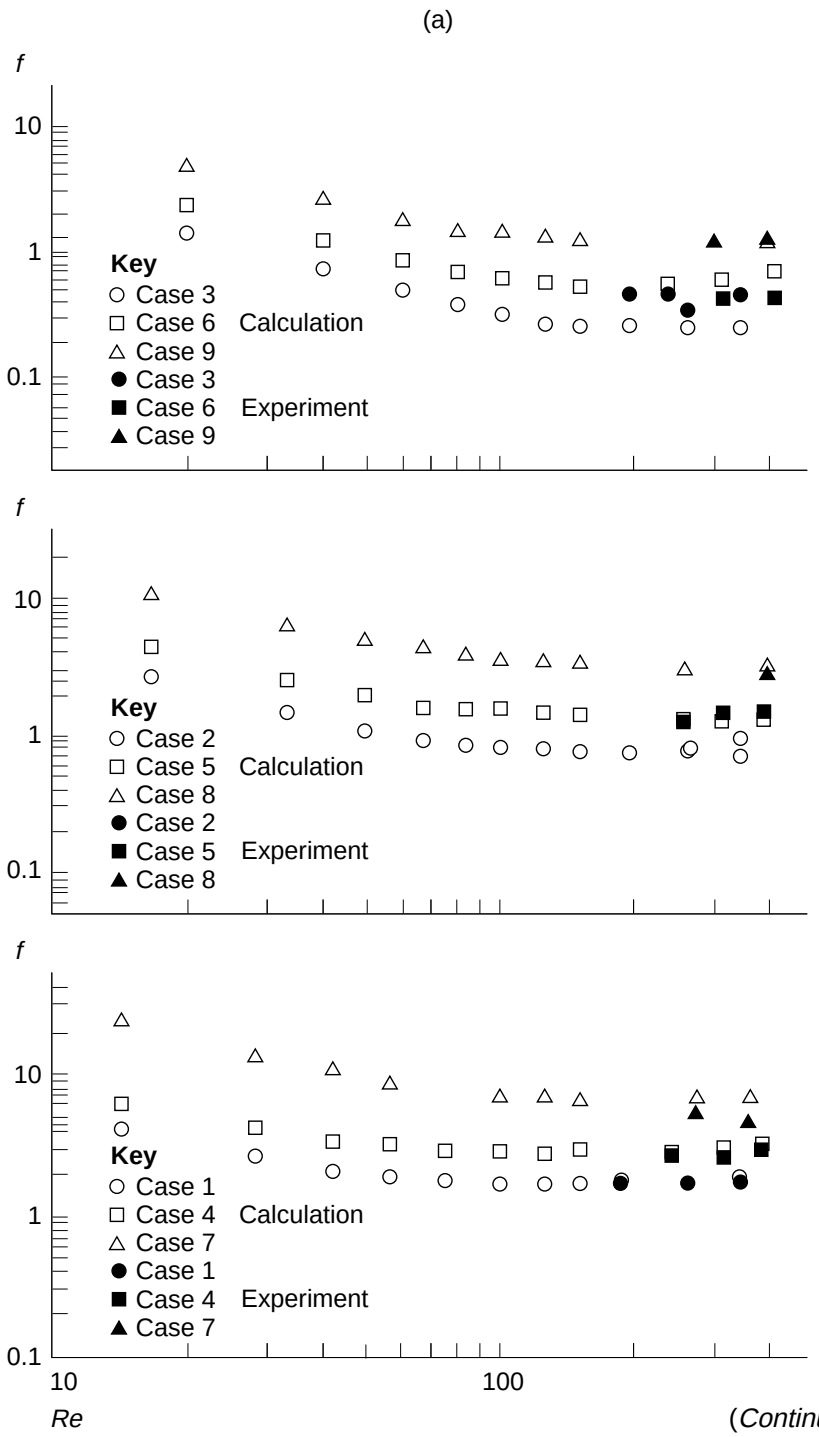

Figure 8.
Calculated results of friction factor, (a) effect of the transverse pitch on heat transfer; (b) effect of the ratio of successive plate length on heat transfer

(*Continued*)

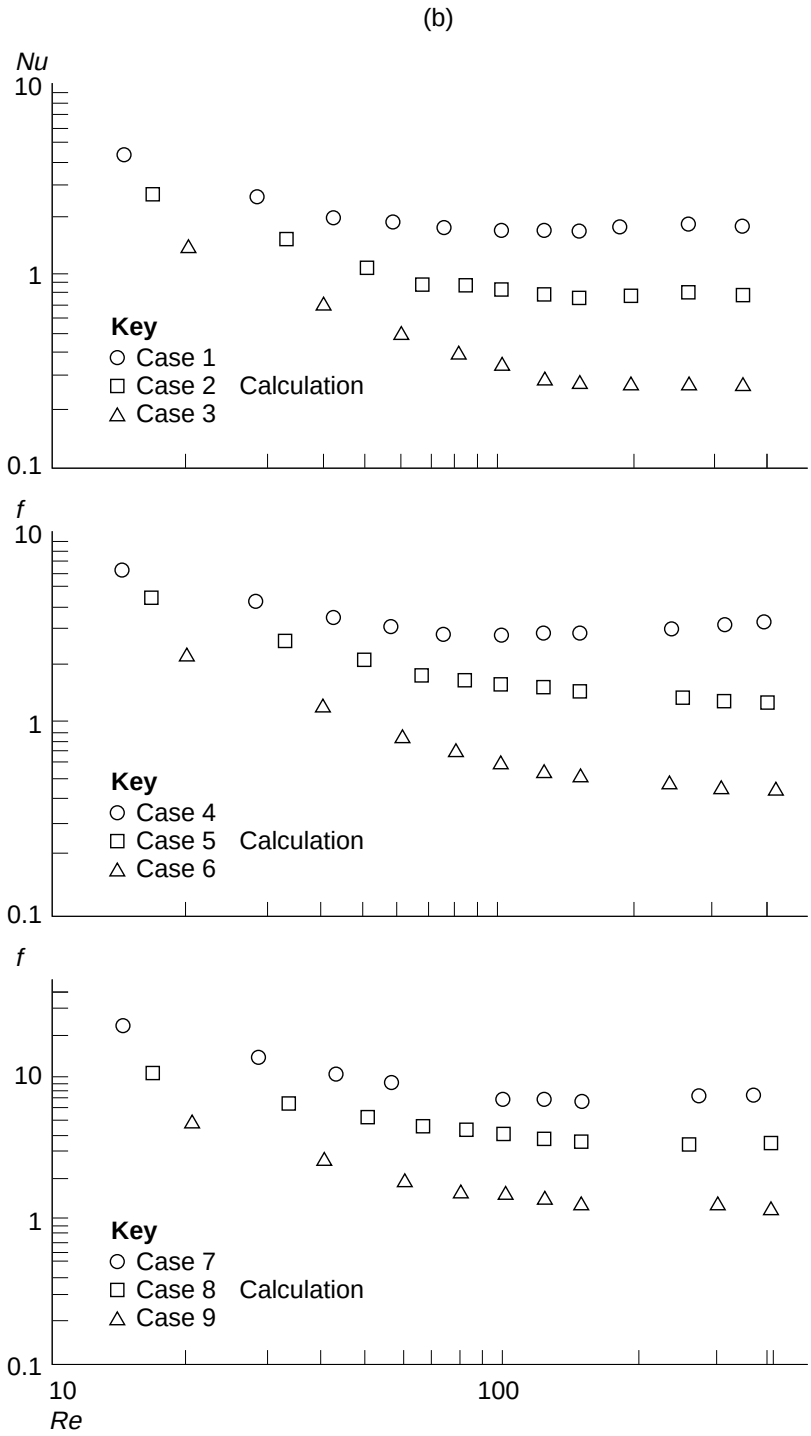
(b)
Nu
10
1
0.1
Key
Case 1
Case 2
Case 3
Calculation
f
10
1
0.1
Key
Case 4
Case 5
Case 6
Calculation
f
10
1
0.1
Key
Case 7
Case 8
Case 9
Calculation
10
100
Re

Figure 8.

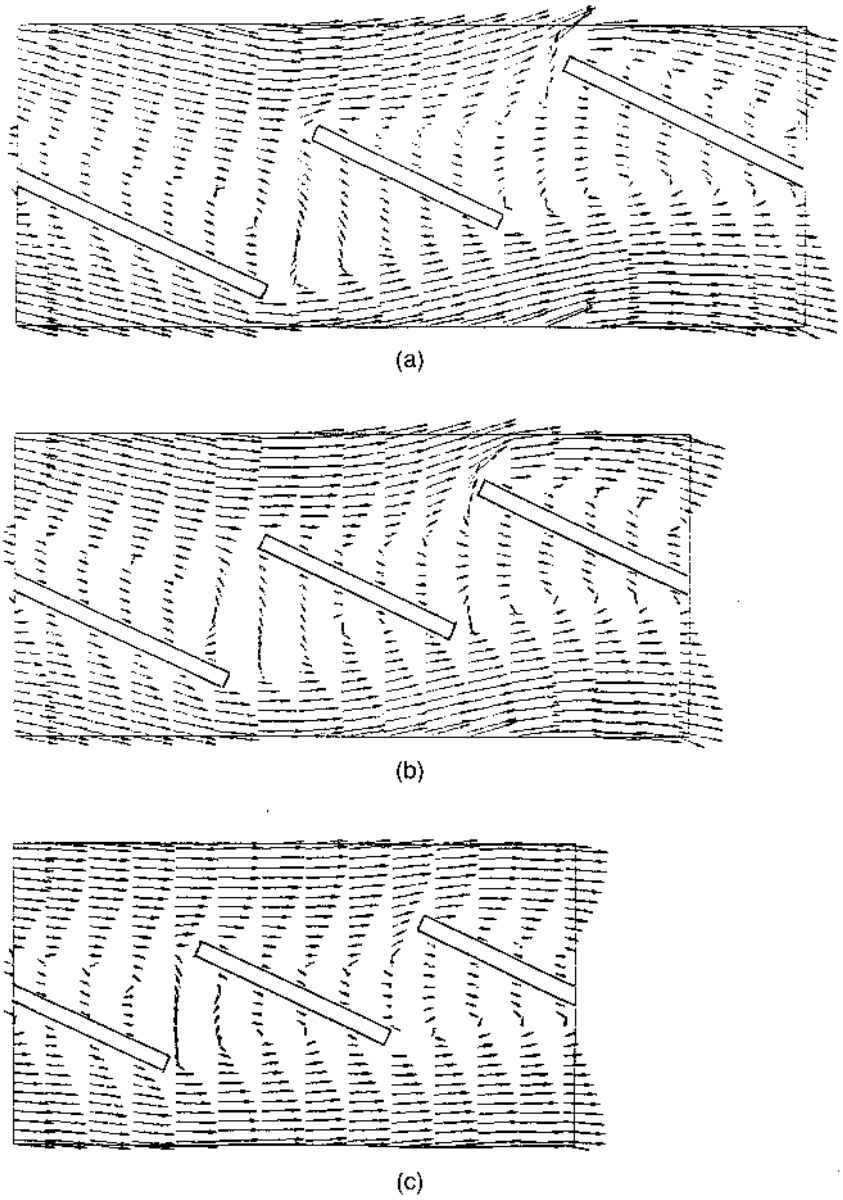

Figure 9.
Velocity fields for (a) Case number 7, $Re = 1.0 \times 10^2$; (b) Case number 8, $Re = 1.0 \times 10^2$; (c) Case number 9, $Re = 1.0 \times 10^2$

Fortunately, the upper limit of the Reynolds number range in the present study is overlapped with the lower limit of the Reynolds number range in the experimental work conducted by Huang and Tao (1993); therefore, comparisons in Nusselt number and friction factor have been made within this overlapped Reynolds number range. The numerically predicted Nusselt

number of the nine cases was compared with the values calculated by using the empirical equation presented by Huang and Tao (1993). The values of the friction factor were taken from the data presented in the thesis of Huang (1990). These experimental results are presented in Figure 7a and Figure 8a by the black symbols. The agreement between the computed *Nu* and *f* values and the experimental results should be regarded to be from reasonably good to moderately good. The average deviation of the predicted Nusselt number from the experimental correlation is –27.8 per cent, while that of the friction factor ranges from +12.3 per cent to –19.3 per cent. For the total of 23 heat transfer data compared, the maximum deviation in *Nu* is –35.3 per cent and that of *f* is 45 per cent. The deviations between the numerical and experimental results may be attributed to the following reasons. From the numerical side, the step-wise method was used to simulate the obliquely positioned plate in the flow field in this paper. As indicated by Rodi *et al.* (1989), the near wall regions may not be resolved very well by the step-wise simulation. From the experimental side, the accurate measurement of flow rate and pressure drop at low Reynolds number is rather difficult and, hence, the measurement uncertainty involved in the low flow rate region may be relatively large. To the authors' knowledge, for the simulation of fluid flow and heat transfer in interrupted plate passage, 10-20 per cent deviation between experimental and numerical results in the low Reynolds number region should be judged to be quite satisfactory. For the interrupted plate array aligned parallel to the flow direction, the disagreement between the experimental and numerical results conducted by Patankar and Prakash (1981) was mainly within this range.

Concluding remarks

The results presented in this paper are the numerical analyses for the heat transfer and fluid flow characteristics of an array of non-uniform plate length, aligned at angles to the air flow direction. Two computational domains are adopted for the prediction of the periodically fully developed fluid flow. To implement the periodic boundary condition for the one-cycle computation domain, linear interpolation technique is proposed. This technique has been proved efficient in that not only the numerical results agree well with the solution obtained in the extended domain, but also its convergence rate is much faster than that with an extended domain, usually with a factor of two. It has been found that both the Nusselt number and the friction factor increase with the increase in L_1/L_2 and T_p/L_p. Comparison of the numerically predicted Nusselt number and friction factor with the relevant experimental results was performed. The agreement should be judged to be from reasonably good to moderately good.

References

Amano, R.S. (1985), "A numerical study of laminar and turbulent heat transfer in a periodically corrugated wall channel", *ASME Journal of Heat Transfer*, Vol. 107, pp. 564-9.

Asako, Y. and Faghri, M. (1986), "Heat transfer and fluid flow analysis for an array of interrupted plates, positioned obliquely to the flow direction", *Proceedings of the Eighth International Heat Transfer Conference*, pp. 421-7.

Hiramatsu, M. and Kajino, M. (1986), "Research and improvement of automotive radiators internal combustion engine", (in Japanese), Vol. 25, pp. 21-8.

Huang, H.Z. and Tao, W.Q. (1993), "An experimental study on heat/mass transfer and pressure drop characteristics for array of non-uniform plate length positioned obliquely to the flow direction", *ASME Journal of Heat Transfer*, Vol. 115, pp. 568-75.

Lee, Y.N. (1986), "Heat transfer and pressure drop characteristics of an array of plates aligned at angles to the flow in a rectangle duct", *International Journal of Heat Transfer*, Vol. 29, pp. 1553-63.

Lee, Y.N. (1989), "Heat transfer and pressure drop characteristics of an assembly of partially segmented plates", *ASME Journal of Heat Mass Transfer*, Vol. 111, pp. 44-50.

Pang, K., Tao, W.Q. and Zhang, H.H. (1990), "Numerical analysis of fully developed fluid flow and heat transfer for arrays of interrupted plates positioned convergently-divergently along the flow direction", *Numer. Heat Transfer,* Part A, Vol.18, pp. 309-42.

Patankar, S.V. (1980), *Numerical Heat Transfer and Fluid Flow*, Hemisphere, Washington, DC.

Patankar, S.V. and Prakash, C. (1981), "An analysis of the effect of plate thickness on laminar flow and heat transfer in interrupted-plate passages", *International Journal of Heat Mass Transfer,* Vol. 24, pp. 1801-10.

Patankar, S.V., Liu, C.H. and Sparrow, E.M. (1977), "Fully developed flow and heat transfer in ducts having streamwise-periodic variation of cross-sectional area", *ASME Journal of Heat Transfer,* Vol. 39, pp. 180-86.

Ridi, W., Majumdar, S. and Schonung, B. (1989), "Finite volume method for two-dimensional incompressible flows with complex boundaries", *Computer Methods in Applied Mechanics and Engineering,* Vol. 75, pp. 369-92.

Sparrow, E.M. and Liu, C.H. (1979), "Heat transfer, pressure drop and performance relationships for in-line, staggered and continuous plate heat exchanger", *International Journal of Heat Mass Transfer*, Vol. 22, pp. 180-86.

Sparrow, E.M., Baliga, B.R. and Patankar, S.V. (1977), "Heat transfer and fluid flow analysis of interrupted-wall channel, with application to heat exchanger", *ASME Journal of Heat Transfer,* Vol. 99, pp. 4-11.

Xin, R.C. and Tao, W.Q. (1988), "Numerical prediction of laminar flow and heat transfer in wavy channels with uniform cross sectional area", *Numer. Heat Transfer*, Vol. 14, pp. 465-81.

Yang, M. and Tao, W.Q. (1992), "A numerical study of natural convection heat transfer in a cylindrical envelope with internal concentric slotted hollow cylinder", *Numer. Heat Transfer,* Part A, Vol. 22, pp. 289-305.

Zhang, H.H. and Lang, X.S. (1989), "The experimental investigation of oblique angles and interrupted plate lengths for louvred fins in compact heat exchanger", *Experimental Thermal and Fluid Science,* Vol. 2, pp. 100-06.